I&EC research
Industrial & Engineering Chemistry Research



Article

# Robust Adaptive Predictive Fault-Tolerant Control Integrated To a Fault-Detection System Applied to a Nonlinear Chemical Process

David Zumoffen, Marta Basualdo, Mario Jordn, and Alejandro Ceccatto

*Ind. Eng. Chem. Res.*, **2007**, 46 (22), 7152-7163 • DOI: 10.1021/ie070019b

# Robust Adaptive Predictive Fault-Tolerant Control Integrated To a Fault-Detection System Applied to a Nonlinear Chemical Process

**David Zumoffen,[†] Marta Basualdo,*[,†] Mario Jordán,[‡] and Alejandro Ceccatto**

*Centro Internacional Franco Argentino de Ciencias de la Información y Sistemas (CIFASIS) (CONICET-UNICAM III-UNR), Bv. 27 de Febrero 210 Bis, S2000EZP Rosario, Argentina*

Most of the control schemes for chemical plants are developed under the assumption that the sensors and the actuators are free from faults. However, the occurrence of faults will cause degradation in the closed-loop performance, having an impact on safety, productivity, and plant economy. In this work, the main novelty is given by the enhancement produced through the integration of the fault detection and identification (FDI) system over a robust adaptive predictive control (RAPC) strategy specially thought to turn it as a fault-tolerant control (FTC) scheme. Additionally, the FDI itself is original because of the sensor and actuator faults treatment. The biases in sensors are detected and quantified by using wavelet decomposition and the extra delays in actuators by applying online identification techniques to appropriately modify the controller action. It is important to remark that the extra time delay, detected particularly at the actuators, is a problem that occurs frequently in practice; however, the academic community has mostly omitted it up to now. This methodology can improve the overall performance for nonlinear stable plants because the FDI is specifically designed as a complement of those aspects that RAPC cannot handle at all. The control technique involves a commutation of a linear time-varying robust filter in the feedback path of the control loop in synchronization with an adaptive predictive controller. Through simulation studies of a continuous stirred tank reactor (CSTR) with jacket, where the integration between FDI and FTC has been implemented, it can be shown that the proposed methodology leads to significant improvement in comparison with the same control scheme without FDI, particularly when the fault magnitude increases.

## 1. Introduction

The rising demands of product quality, effectiveness, and safety in modern industries have encouraged the research on fault diagnosis for dynamic systems. It has received more and more attention and has developed quickly in the past three decades. Most of the works in the literature only analyze the design problem of the fault diagnosis system (FDS). Generally, these works are focused in the monitoring systems design without considering any integration with the control policy. In general, the FDS allows the detection and isolation of changes in the process states that can arise by faulty behavior in the process components (sensors, actuators, etc.) and/or by disturbances. The FDS developed in this work belongs to the category of process history based according to the classification given by Venkatasubramanian et al.[1−3] Two specific faults, such as a bias at the sensor and an extra time delay at the actuator, were chosen. While the former was largely studied,[4] the latter was only tackled by a few people, even when time delay exists widely in practice,[5] specially in many chemical processes where they are induced by a great number of reasons. They might cause control performance deterioration up to closed-loop instability. Because of this, in the work described in this paper, it is considered that the development of fault-diagnosis methods for systems with time delay is very important to analyze. In this context, Wei et al.[6] discussed an adaptive predictive control based on transfer function model continuously updated by means of plant−model error minimization via regressive methods, addressed in the variable-delay problem. Another approach to overcome the multiple discrete time delays in both states and outputs is presented by Jiang and Zhou[7] where the fault detection and identification system (FDIS) is based on an adaptive observer.

The study of fault-tolerant control (FTC) for nonlinear time-varying systems is still an open problem and has become a very active research topic for both theoretical and practical reasons. Since the faults are obviously time varying, it becomes natural to study FTC in this context. Traditionally, FTC methods have been classified into two categories:[8] the first group is based on fault detection and isolation and the second one is independent of fault diagnosis (active and passive methods, respectively). Recently, different strategies appeared in the literature that can overcome the classical conflict between performance and robustness in the traditional feedback framework. Campos-Delgado and Zhou[9] proposed an FTC strategy from a robust control perspective by applying the recently introduced generalized internal model control (GIMC) architecture. The authors proposed an FTC design consisting of two parts: a nominal performance controller and a robustness controller, working in such a way that, when a sensor failure is detected, the controller structure is reconfigured by adding a robustness loop to compensate the fault. The commutation between two controllers is carried out by measuring the plant−model filtered error.

Few works that present a link between FDS and FTC for chemical processes can be found; one of them is by Tao et al.,[10] where the problem of adaptive compensation for actuator failures is addressed. Zhang et al.[11] presented a methodology for integrating both FDS and FTC by using two fault-tolerant controllers designed under backstepping and adaptive techniques. Another integrated fault detection (FD) and FTC approach can be found by El-Farra;[12] it is able to handle both

* To whom correspondence should be addressed. Tel.: +54-341-4821771-104. Fax: +54-341-482-1772. E-mail: basualdo@ifir.edu.ar.

[†] Universidad Tecnológica Nacional, Facultad Regional Rosario.

[‡] Instituto Argentino de Oceanografía (IADO-CONICET), Dto. de Ing. Eléctrica y de Computadoras Universidad Nacional del Sur, Bahía Blanca, Argentina.

10.1021/ie070019b CCC: $37.00 
Published on Web 10/02/2007

constraints and control actuator faults. In that case, different tools are considered such as state feedback, FD based on a reduced-order model, spatially distributed feedback, and supervisory control. All these strategies support an appropriate switching between different actuator configurations in the event of faults by means of control reconfiguration logic. The proposed approach is applied to a diffusion−reaction process. More recently, Patwardhan and co-workers[13,14] presented a model predictive control (MPC) algorithm integrated with a model-based FDS. A complete state estimator development is proposed for multivariable systems[13] in which unknown dead time and nonmeasured disturbances are considered. The proposed strategy is based on generalized orthonormal basis filters (GOBF), and new off-line estimation algorithms are implemented. Thus, the optimal state estimator can be directly used in both MPC and FDS. The approach is applied to the benchmark shell control problem as well as to an experimental pilot plant. Patwardhan et al.[14] presented a reformulated version of a previous multivariable FTC design.[15] There, the control algorithm is based on MPC and the FDS is implemented using the generalized likelihood ratio (GLR) principle. The controller as well as the FDS are designed based on the state-space model identified using the algorithms developed in a previous work[13] and the GOBF strategy. In these last works, bias in sensors and actuators are considered as common faults.

In this work, a new FTC strategy to compensate specific faults effects and to improve the overall performance for nonlinear stable plants is applied. The FTC approach involves a commutation between a linear time-varying robustness filter in the feedback path of the control loop and an adaptive predictive controller (APC). The decision of which of both modes has to work is based on specific indicators that will be described in the following sections. They are closely related to the operation conditions, which are checked every sampling time. This strategy is developed in a modular way composed by two stages. On one side, the good asymptotic performance of the APC system is reached. On the other side, the adaptive robustness filter (APRF) is accounted if sudden dynamic changes affect significantly the closed-loop behavior and APC cannot achieve good performance in these cases. The principal advantage of using this methodology is that a stable asymptotic behavior without extra tuning parameters is always achieved. The convergence and stability of the control system is analyzed in detail by Jordán and co-workers.[16,17] However, if the faults significantly change the system dynamics, the speed of adaptation may be inadequate. By taking this into account, the faults presented here have been chosen as those that cannot be handled well by that control structure. In this context, it is thought that the integration with the FDI would ensure a real improvement for the overall system. For example, a bias at the sensor cannot be detected by any controller, classical or advanced. Another important problem to be solved is the variable time delay in control loops. It affects the control performance, causing instability, and loses in product quality. Therefore, with the help of the FDS, the FTC will work more actively and effectively. The faults in the process elements are characterized by an abrupt bias measurement for sensors and an extra time delay in the control loop for actuators; unmeasured disturbances are also accounted. The FDS design is based on signal processing topics such as the wavelet transform and the recursive dead-time estimation. The sensor faults are recognized by a novel robust wavelet processing approach that is useful to detect and estimate the fault based on a multiresolution filtering. In this case, a set-point compensation is generated. For time delay, the online estimation method, known as the explicit time-delay parameter,[18] is proposed based on an autoregressive with exogenous input (ARX) discrete model[19] used for emulating the actuator behavior. To compensate this fault, the controller parameters must be updated online according to the correct value estimated by this identification methodology. Several tests have been done on a continuous stirred tank reactor (CSTR) with jacket. The selected simulation results are presented as an indicator of the effectiveness of the proposed strategy.

## 2. Online Approximation-Based Adaptive Predictive Control With Robust Filter

**2.1. Adaptive Predictive Approach.** Consider a single-input, single-output system with linearizable dynamic for every operation point in the working region. Therefore, the predictive controller structure can be obtained by minimizing the energy criterion in eq 1 applied at every step $k$.

$$J(k) = \sum_{i=N_1}^{N_2} \alpha_i^2 e^2(k+i) + \sum_{i=0}^{N_u-1} \beta_i^2 \bar{u}^2(k+i) \tag{1}$$

where $e(k)$ is a tracking error between a desired trajectory $y_r(k)$ and the predicted system output $\hat{y}(k)$ evaluated on a so-called prediction horizon $[N_1, N_2]$ via model, $y(k)$ and $u(k)$ are the past values of the system output and control action, respectively, and $\bar{u}(k)$ is the future control action calculated over the so-called control horizon $[0, N_u - 1]$. Equation 1 can be accompanied with restrictions on $y(k)$ and $u(k)$. The future output trajectory is originally calculated by means of a FIR model (finite impulse response: $\hat{g}(i)$, $i = 1, ..., N$) of the system. The optimal control sequence $\bar{u}(k)$ can be easily deduced for the unconstrained case by searching for the global minimum of $J(k)$ with respect to $\bar{u}(k)$ over $N_u$. Because the functional of eq 1 is quadratic, the minimum can be analytically calculated as a linear optimization problem without restrictions.

Considering the FIR model and the process operation point $[u_{00}, y_{00}]$, the model prediction of the plant can be expressed as it is presented in eq 2.

$$\begin{aligned}\hat{y}(k+i) &= \sum_{j=1+d}^{N} \hat{g}(j)[u(k+i-j) - u_{00}] + y_{00} + \hat{\eta}(k+i) \\ &= \sum_{j=1+d}^{N} \hat{g}(j)u(k+i-j) + c\hat{g}l + \hat{\eta}(k+i)\end{aligned} \tag{2}$$

where $u(k+i)$ is the control signal, $\hat{y}(k+i)$ is the model prediction, $\hat{\eta}(k+i) = y(k) - \hat{y}(k)$ is the plant−model mismatch (disturbances estimation), and $c\hat{g}l = y_{00} - \sum_{j=d+1}^{N} \hat{g}(j)u_{00}$ is the plant parameter, for $i = N_1...N_2$.

The tracking error vector (eq 3) in the prediction horizon can be expressed using the future and past actions control vectors, eqs 6 and 7, respectively.

$$\mathbf{e}(k) = \mathbf{y}_r(k) - \hat{\eta}(k) - \mathbf{T}_1\mathbf{G}\mathbf{T}_2\bar{\mathbf{u}}(k) - \mathbf{T}_3\mathbf{S}\mathbf{T}_4\psi(k) \tag{3}$$

with

$$\mathbf{y}_r(k) = [y_r(k+N_1), \cdots, y_r(k+N_2)]^T \tag{4}$$

$$\hat{\eta}(k) = [1, \cdots, 1]^T(y(k) - \hat{y}(k)) \tag{5}$$

$$\bar{\mathbf{u}}(k) = [u(k), \cdots, u(k + N_u - 1)]^{\mathrm{T}} \tag{6}$$

$$\psi(k) = [u(k-1), \cdots, u(k - N + N_1)]^{\mathrm{T}} \tag{7}$$

and

$$\mathbf{G} = \begin{bmatrix} \hat{g}(1) & 0 & \dots & 0 \\ \hat{g}(2) & \ddots & \ddots & \vdots \\ \vdots & \ddots & \hat{g}(1) & 0 \\ \hat{g}(N) & \ddots & \hat{g}(2) & \hat{g}(1) \\ 0 & \ddots & \vdots & \hat{g}(1) + \hat{g}(2) \\ \vdots & \ddots & \hat{g}(N) & \vdots \\ 0 & \dots & 0 & \sum_1^N \hat{g}(i) \end{bmatrix} \tag{8}$$

$$\mathbf{S} = \begin{bmatrix} \hat{g}(2) & \hat{g}(3) & \hat{g}(4) & \dots & \hat{g}(N) \\ \hat{g}(3) & \hat{g}(4) & \vdots & \iddots & 0 \\ \hat{g}(4) & \vdots & \hat{g}(N) & \iddots & 0 \\ \vdots & \hat{g}(N) & \iddots & \iddots & \vdots \\ \hat{g}(N) & >0 & 0 & \dots & 0 \end{bmatrix} \tag{9}$$

The transformation matrices $\mathbf{T}_1$, $\mathbf{T}_2$, $\mathbf{T}_3$, and $\mathbf{T}_4$ allow one to select specific parts of $\mathbf{G}$ and $\mathbf{S}$, and they are functions of the prediction horizon $[N_1, N_2]$, the control horizon $N_u$, and the FIR model order $N$. The matrices $\mathbf{A} = \mathrm{diag}(\alpha_{N_1}, ..., \alpha_{N_2})$ and $\mathbf{B} = \mathrm{diag}(\beta_1, ..., \beta_{N_u})$ are penalty coefficients of the energies of $e(k)$ and $\bar{u}(k)$, respectively.

Using eqs 3 and 7, the functional of eq 1 in the matrix form can be expressed as

$$J(k) = \mathbf{e}^{\mathrm{T}}(k)\mathbf{A}^2\mathbf{e}(k) + \bar{\mathbf{u}}^{\mathrm{T}}(k)\mathbf{B}^2\bar{\mathbf{u}}(k) \tag{10}$$

Then the control structure (control law) can be obtained by means of $\partial J/\partial u = 0$, and considering that only the first component of the optimal future control actions vector will be applied $\bar{\mathbf{u}}(k)$ in this sample time, in eq 11 this control law is expressed in terms of the $z$ variable.

$$D(z^{-1})U(z) = z^{N_1}R(z)Y_{\mathrm{r}}(z) - R(1)(Y(z) - \hat{Y}(z)) \tag{11}$$

where

$$D(z^{-1}) = 1 + d_1 z^{-1} + ... + d_{N-N_1} z^{-(N-N_1)}$$

$$R(z) = r_1 + r_2 z + ... + r_{N_2-N_1+1} z^{(N_2-N_1)} \tag{12}$$

and

$$\begin{bmatrix} d_1 \\ d_2 \\ \vdots \\ d_{N-N_1} \end{bmatrix}^{\mathrm{T}} = [r_1, r_2, ..., r_{N_2-N_1+1}]\mathbf{T}_3\mathbf{S}\mathbf{T}_4 \tag{13}$$

$$\begin{bmatrix} r_1 \\ r_2 \\ \vdots \\ r_{N_2-N_1}+1 \end{bmatrix}^{\mathrm{T}} = [1, 0, ..., 0][\mathbf{T}_2{}^{\mathrm{T}}\mathbf{G}^{\mathrm{T}}\mathbf{T}_1{}^{\mathrm{T}}\mathbf{A}^2\mathbf{T}_1\mathbf{G}\mathbf{T}_2 + \mathbf{B}^2]^{-1}[\mathbf{T}_2{}^{\mathrm{T}}\mathbf{G}^{\mathrm{T}}\mathbf{T}_1{}^{\mathrm{T}}\mathbf{A}^2] \tag{14}$$

From eqs 11, 13, and 14, it is evident that the control law $u(k)$ requires static compensation for achieving zero static error. Then the gain compensation factor $K_{\mathrm{offs}}$ is given by

$$K_{\mathrm{offs}} = \frac{1}{\sum_{i=1}^{N} \hat{g}(i)} \tag{15}$$

A prefilter for smoothing the $w(k)$ reference signal so as to generate a flat reference trajectory $y_{\mathrm{r}}(k)$ is included; a simple algorithm can be used for this purpose (eq 16)

$$y_{\mathrm{r}}(k) = \alpha_{\mathrm{r}} y_{\mathrm{r}}(k-1) + (1 - \alpha_{\mathrm{r}})w(k) \tag{16}$$

where $\alpha_{\mathrm{r}}$ is a smoothing coefficient between 0 and 1, which can handle the closed loop dynamic. $\alpha_{\mathrm{r}}$ is selected close to the limit 0 for achieving a rapid response and vice versa when it is closed to limit 1. Implementing the control structure shown in eq 11 and considering eqs 15 and 16, the control scheme of Figure 1 is obtained.

As can be appreciated from eqs 11−14, this structure is suitable for the design of adaptive controllers. By making an online adaptation of the linear FIR model and rewriting eq 2, the following results

$$\hat{y}(k) = \psi(k)^{\mathrm{T}}\hat{\theta}(k) + \eta(k) \tag{17}$$

where

$$\psi(k) = [u(k-1), ..., u(k-N), 1]^{\mathrm{T}}$$

$$\hat{\theta}(k) = [\hat{g}(1, k), ..., \hat{g}(N, k), c\hat{g}l(k)]^{\mathrm{T}} \tag{18}$$

From eq 18, it can be noted that the parameters vector $\hat{\theta}(k)$ is constituted by two components (augmented form). The vector $[\hat{g}(1, k), ..., \hat{g}(N, k)]$ contains the $N$ FIR coefficients and a scalar $c\hat{g}l(k)$ named the plant parameter for each sampling time $k$. The parameter $c\hat{g}l(k)$ has information of the process operation point $[y_{00}, u_{00}]$ and its modifications. Then the online estimation process allows one to obtain the FIR coefficients and the working point updated simultaneously.

Defining the prediction error $\epsilon(k) = y(k) - \hat{y}(k)$ and minimizing $V = (\sum_1^N \epsilon^2(k))/N$ with respect to $\theta$, the least-square (LS)[19] estimate can be obtained as

$$\hat{\theta}_N^{\mathrm{LS}} = [\sum_{k=1}^{N} \psi(k)\psi^{\mathrm{T}}(k)]^{-1} [\sum_{k=1}^{N} \psi(k)y(k)] \tag{19}$$

This structure allows one to update the estimate $\hat{\theta}$ online, for example, updating in a recursive way the covariance matrix[16,19] $P = U_* D_* U_*{}^{\mathrm{T}}$. As an alternative, it can be implemented by means of the UD-factorization algorithm,

$$\hat{\theta}(k) = \hat{\theta}(k-1) + U_*(k)D_*(k)U_*{}^{\mathrm{T}}(k)\psi(k)\tilde{e}(k)$$

$$\tilde{e}(k) = y(k) - \psi(k)^{\mathrm{T}}\hat{\theta}(k-1)$$

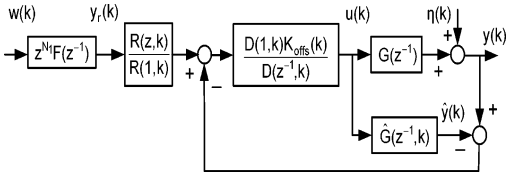


**Figure 1.** Adaptive predictive control (APC) structure.

$$U_*(k) = f_{U_*}(U_*(k-1), \psi(k), \lambda)$$

$$D_*(k) = f_{D_*}(D_*(k-1), \psi(k), \lambda) \tag{20}$$

where $\lambda$ is the forgetting factor, $\tilde{e}(k)$ is an a priori estimation error, and $f_{U_*}$ and $f_{D_*}$ are recursive formulas that will provide $U_*$ and $D_*$, respectively. As a result, both the FIR model and the controller are updated online.

**2.2. Adaptive Predictive Robust Filter Approach.** In the case of a process−model mismatch $\Delta G = G - \hat{G} \neq 0$, the parallel compensation structure provides a direct way to achieve robustness of the closed loop by including a filter in the feedback path. The basic idea consists of making a correction of the predictions given by a nominal FIR model $G_0(z^{-1})$ by means of an adaptive modification. Consider that

$$\hat{G}(z^{-1}, k) = \Delta\hat{G}(z^{-1}, k) + G_0(z^{-1}) \tag{21}$$

where

$$\Delta\hat{G}(z^{-1}, k) = \Delta\hat{g}(1, k)z^{-1} + \cdots + \Delta\hat{g}(N, k)z^{-N} \tag{22}$$

The nominal FIR model $G_0(z^{-1})$ is available by the off-line identification procedure, its coefficients are $g_0(i) = [h(i) - h(i-1)]/\Delta u(k)$, and $h(k)$ is the plant response to a step change in the control signal $u(k)$. This nominal model generates a stable controller ($D_0(z^{-1})$, $R_0(z)$, $K_{\text{offs}}$) and leads to rewriting the FIR model prediction as

$$\hat{y}(k) = \sum_{i=1}^{N} \Delta\hat{g}(i)u(k-i) + \sum_{i=1}^{N} g_0(i)u(k-i) + cgl + \eta(k) \tag{23}$$

Following similar steps as those described in the previous section with an identical structure as appears in eq 17, the same regressor, $\psi(k)$ are obtained, while considering that the estimate parameter vector and the prediction error, in this case, are, respectively, as follows:

$$\Delta\hat{\theta}(k) = [\Delta\hat{g}(1, k), ..., \Delta\hat{g}(N, k), c\hat{g}l(k)]^{\mathrm{T}}$$

$$\epsilon(k) = [y(k) - y_0] - \psi^{\mathrm{T}}(k)\Delta\hat{\theta}(k) \tag{24}$$

Then, applying the recursive algorithm (eq 20) again, an online model updating for the robust filter is available $\Delta\hat{G}(z^{-1})$.

Under these conditions, the static compensation must be

$$K_{\text{offs}}(k) = \frac{1}{(\Delta\hat{G}(1, k) + G_0(1))} \tag{25}$$

This control strategy is initially based on a stable nominal controller, obtained from the nominal stable FIR model $G_0(z^{-1})$ identified off-line. By accounting eqs 23−25 and 11, the control structure shown at Figure 2 can be implemented.

The asymptotic performance of the adaptive control system is, in general, better than that obtained by a robust filter system, mainly if the particular tuning coefficients allow the adaptive control to guarantee asymptotic steady-state stability. Therefore, if sudden dynamic changes affect significantly the closed-loop response behavior, they may be much more efficiently damped down by a robust-filter system. Additionally, an asymptotically stable and good performance behavior is achievable without extra tuning parameters. It must be noted that a suitable synchronization of both approaches is useful in order to share the manifested advantages of both modes.[16]

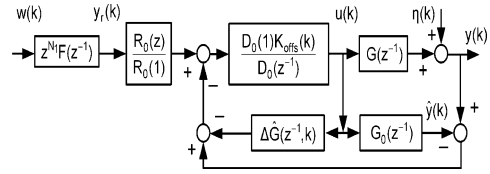


**Figure 2.** Adaptive predictive robust filter (APRF) structure.

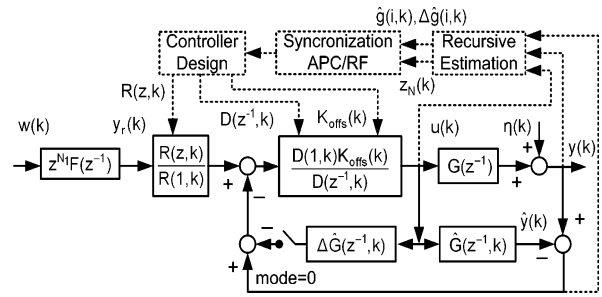


**Figure 3.** Adaptive predictive control with robustness filter (APCWRF) structure.

**2.3. Adaptive Predictive Control With Robust Filter.** In order to improve the performance, a proper synchronization between both the adaptive predictive control and the adaptive robust filter approaches has to be done. It is carried out by means of an appropriate indicator function (mode) that enables the commutation between both algorithms automatically. It is schematically presented at Figure 3.

It is well-known that adaptive control systems may suffer from long-term instability when the manipulated variable $u(k)$ is not rich enough in order to ensure a good persistent excited regressor $\psi(k)$ in the space $\mathscr{R}^N$. In order to supervise this probable misbehavior, the use of proper indicators is recommended in case it would be necessary to stop the estimation at any time. For instance, the eigenvalues evolution of $U_*(k)D_*(k)U_*^{\mathrm{T}}(k)$ or $D_*(k)$ is found to be suitable to detect a future degradation of the estimates $\hat{\theta}(k)$. Another useful indicator is the real variable[16,20]

$$z_N = \frac{\lambda}{\lambda + \psi^{\mathrm{T}}(k)U_*(k-1)D_*(k-1)U_*^{\mathrm{T}}(k-1)\psi(k)} \tag{26}$$

where $0 \leq z_N \leq 1$, indicating a good excited system when it is close to 0 and a poorly excited system when it is next to 1. In addition, the second indicator defined as it is shown in eq 27 is very useful[16,20]

$$S_1(k) = \begin{Bmatrix} 0.7S_1(k-1) + 0.3z_N^2(k), & \text{if } S_1(k-1) \leq 0.8z_N(k) \\ 0.99S_1(k-1) + 0.01z_N^2(k), & \text{in another case} \end{Bmatrix} \tag{27}$$

Finally, a set of equations is accounted that is able to detect the excitation richness and, thus, to make a determination with respect to updating (or not) the vector of parameters. In addition, a supervision of the control loop stability in adaptive predictive

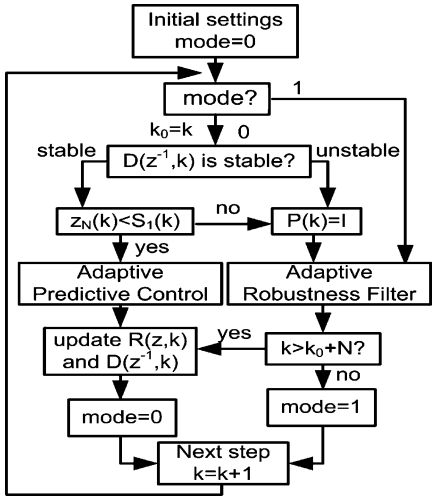


**Figure 4.** APCWRF synchronization algorithm.

control mode must be done. It can be made by analyzing the roots of the polynomial $D(z^{-1}, k)$ at each sampling time. Thus, a complete set of conditions for developing the synchronization rule is available.

In Figure 4, a representative flow chart of how the synchronization algorithm works is shown. The binary variable mode indicates which control algorithm must be executed. For each step time, the mode variable is analyzed; mode = 0 indicates that the APC approach was executed in the previous step time, before the stability of the controller $D(z^{-1}, k)$ is evaluated by following this approach. In the stable case, the excitation degree is checked through condition $z_N(k) < S_1(k)$, and if it is true, the APC approach is run again in the next sampling time and the controller matrices are updated. On the other hand, if the polynomial $D(z^{-1}, k)$ is unstable or the excitation degree is not enough, the APC algorithm is switched off and the APRF approach begins working with the mode = 1 indicating this situation. The APRF algorithm runs during a determined time ($N$ samples) before returning to the APC approach and updating the controller matrices. The recursive estimation of the complete FIR model is avoided in the case of poor excitation degree; under this condition, APRFC is switched on. In the APRF method, a nominal stable controller is used together with the nominal FIR model (both computed off-line). In this case, the recursive estimation of the model residuals is always made without considering the excitation degree, since minimal modifications around the nominal FIR model are produced. The interconnection of the two methods is carried out as is shown in Figure 4.

## 3. Case Study: CSTR With Jacket Process

The system studied[21] consists of a constant-volume, constant-density, cooled CSTR with a first-order, irreversible reaction A → B. Even though this model is quite simple, it contains most of the relevant issues surrounding an open-loop, nonlinear reactor. In Figure 5 can be appreciated the control strategy for the mentioned plant; this system is rigorously modeled by one component balance and one energy balance,

$$\frac{dC_A}{dt} = -k_0\, e^{-P/T_1} C_A + \frac{F_{inA}}{V_1}(C_{inA0} - C_{inA}) \qquad (28)$$

$$\frac{dT_1}{dt} = k_1\, e^{-P/T_1} C_A + \frac{F_{inA}}{V_1}(T_{inA} - T_1) + \frac{Q_{JP}}{\rho_P c_P V_1} \qquad (29)$$

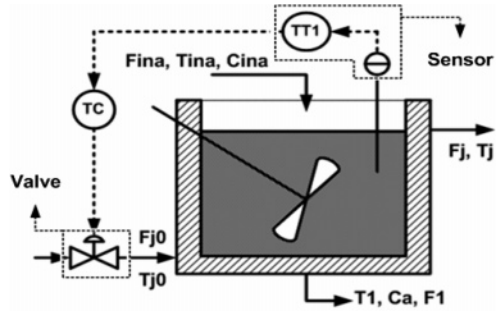


**Figure 5.** CSTR with jacket process.

**Table 1. Variables in CSTR with Jacket Process**

| variables | definition | units |
|---|---|---|
| $F_{inA}$, $F_{J0}$, $F_J$, $F_1$ | flows | $m^3/s$ |
| $T_{inA}$, $T_{J0}$, $T_J$, $T_1$ | temperatures | K |
| $C_{inA}$, $C_A$ | concentrations | $mol/m^3$ |

and the energy balance for the jacket,

$$\frac{dT_J}{dt} = \frac{F_{J0}}{V_J}(T_{J0} - T_J) - \frac{Q_{JP}}{\rho_J c_J V_J} \qquad (30)$$

where $Q_{JP}$ is the interchanged heat. The definitions of the variables are given in Table 1. The control structure keeps the reactor temperature ($T_1$) (controlled variable) under a specific range by manipulating the coolant flow to the jacket ($F_{J0}$). Therefore, the $C_A$ composition is indirectly controlled since it has a strong relationship with $T_1$. In addition, the disturbance variables such as $C_{inA}$, $T_{inA}$, and $F_{inA}$ (concentration, temperature, and flowrate of reactant A, respectively) can vary during the time and could produce several changes in the plant operation point. In the paper by Primucci and Basualdo[21] can be found more details about this process.

## 4. Fault-Diagnosis System Design

The most common faults in a chemical process can be defined as several types of malfunctions in actuators and/or sensors. Both of them are considered here, such as a bias at the sensor and extra time delay at the actuator. The reason for this choice is because time delay exists widely in practice induced by long-distance transportation and communication or mechanical faults in valves. Another reason for this selection is because it might cause the closed-loop systems instability and control performance deterioration, so the FTC represents a valuable tool for support for these kind of abnormal events. However, only a few works analyze these type of faults. The (APC) algorithm working without the FDS cannot modify the controller matrix sizes, in the presence of the extra delays in the closed loop, so stability cannot be guaranteed for this faulty behavior. In order to handle this problem, it is necessary to update the controller parameters such as the prediction horizon online, particularly the beginning of the prediction horizon $N_1$. Therefore, the size of the transformation matrices $\mathbf{T}_1$, $\mathbf{T}_2$, $\mathbf{T}_3$, and $\mathbf{T}_4$ are modified properly according to the right estimated time delay.

On the other hand, a common problem reported in sensors is when an abrupt offset appears in a specific measurement. This kind of fault in the controlled variable measurement can generally be compensated in order to achieve zero tracking error. Obviously, this incorrect measurement affects the process by modifying the normal operation point. The APC and APC with robustness filter(APCWRF) approaches do not have any way to detect and avoid this fault propagation into the process. An alternative for solving this problem is an additive compensation

at the set-point policy, for which sign and magnitude are provided by the FDS. This correction could be done on the measurement; in any case, the results are absolutely the same.

Hence, the proposed FDS is thought to provide the precise information about the type, time, and magnitude of each fault expected to occur. This information is accounted for by doing the proper control configuration in order to make it fault tolerant.

**4.1. Valve Fault Detection and Estimation.** The dead-time detection in process (or time-delay estimation, TDE) is a widely studied problem. During the last few years, several strategies with different performances have arisen according to the application cases. These methods can be classified as follows: (1) time-delay approximation model, (2) explicit time-delay parameter, (3) area and moment, and (4) higher-order statistics (HOS).[18]

It must be noted that the FIR adaptive model, described in previous sections, is updated just under specific conditions when the APC algorithm is active. It is thought to capture the existing process nonlinearities between the reaction temperature (output) and the coolant incoming flow (input) to the jacket. Otherwise, when APRF is working, the FIR nominal model (not adaptive) is adopted and $\Delta G$ accounts for a range of possible plant variations. The input−output delay in this control loop could be estimated directly from the FIR coefficients updated by the thresholding approach. Using this strategy, several problems exist:

- The delay estimation is poor and would produce both false detection and misdetection.
- The fault detection instant is very influenced by the convergence time of the recursive estimation algorithm.
- The identified delay cannot be adjudged to the actuator only. It could be produced by other elements in the loop such as the transmission lines, the sensors, and the process itself.

It is clear that, independently of which of both modes are working, the correct estimation of the extra delay caused by a faulty behavior needs to be done with the help of the FDS. Therefore, it justifies the need for this system designed to compensate these specific faults and working externally to the control scheme.

In order to efficiently detect the extra time delay at the actuator, the autoregressive with extra input (ARX) valve model is developed.[19] This model ties the control signal (input) and the measured coolant flow (output). When the valve works normally within a specific range, it behaves approximately as a linear system and obviously facilitates the monitoring and estimation tasks. The estimated delay, provided by the ARX model, is used for updating the controller matrix dimensions, avoiding stability problems.

The dead-time estimation is done based on the methodology cited as explicit time-delay parameter. The discrete model of the valve is given by eq 31; $y(k)$ is the measured coolant flow, $u(k)$ is the control signal calculated by the controller algorithm, and $\hat{y}(k)$ is the coolant flow estimated by the ARX model.

$$G_{vm}(z^{-1}) = \frac{b_1 + b_2 z^{-1} + \cdots + b_{n_b} z^{-n_b+1}}{1 + a_1 z^{-1} + \cdots + a_{n_a} z^{-n_a}} z^{-d} \tag{31}$$

where $n_a$ and $n_b$ are the orders of the denominator and the numerator, respectively, and $d$ is the delay present in the input−output model. The off-line least-squares identification process using the ARX model can be carried out by expressing the output prediction in the linear regression form

$$\hat{y}(k) = -\sum_{i=0}^{n_a} a_i y(k-i) + \sum_{i=1}^{n_b} b_i u(k-i+1-d) = \psi^T(k)\theta \tag{32}$$

where

$$\theta = [a_1, a_2, \cdots, a_{n_a}, b_1, b_2, \cdots, b_{n_b}]^T \tag{33}$$

$$\psi(k) = [-y(k-1), -y(k-2), \cdots, -y(k-n_a), u(k-d), u(k-1-d), \cdots, u(k-n_b+1-d)]^T \tag{34}$$

Then the least-square estimate, as shown in eq 19 but now using the regression model of eqs 33 and 34, can be found. The model employed here has been selected, with $n_a = 1$, $n_b = 1$, and $d = 0$, obtaining the following parameters: $a_1 = 0.0067$ and $b_1 = 0.9933$. In the identification procedure, it used historical data under normal conditions (zero delay).

It is assumed that the faulty valve operation only modifies the delay between input and output. The objective of this method is to make an online search over all the possible discrete dead times in a moving temporal window named $N_w$. It tries to minimize the mean-square error between the valve output and the model prediction (eq 35). The moving temporal window $N_w$ allows one to evaluate the cost function and to perform the online delay search using the valve model. Any modification in the valve delay is detected only in the transient response (set-point changes or disturbance rejection) analyzing the data from the actual time up to the previous $N_w$ samples.

$$V(k) = \frac{1}{N_w} \sum_{i=1}^{N_w} [F_{J0}(k-i) - G_{vm}(z^{-1}, d)u(k-i)]^2 \tag{35}$$

where

$$G_{vm}(z^{-1}, d) = \frac{b_1 z^{-d}}{(1 + a_1 z^{-1})} \tag{36}$$

is a possible model set assuming that the remaining parameters of the model do not change. By means of the discrete valve model, a continuous monitoring is performed. Thus, any modification in the true delay of the valve is detected, estimated, and reported on line. This approach allows the development of an effective FDS able to help with properly adapting the controller parameters, such as the prediction horizon $N_1$, which is crucial in the closed-loop stability issue. It is updated by an additive compensation based on the delay estimation given by the FDS measured at samples when the criteria $V(k)$ in eq 35 is minimized over $N_w$. This moving temporal window has been adopted for the CSTR example equal to 200 samples for both APC and APCWRF approaches.

**4.2. Sensor Fault Detection and Estimation.** This fault is characterized by an abrupt change in the measurement, which is seen by the controller as a disturbance effect. Therefore, this kind of sensor fault only can be detected in the transient response. So, it is necessary to design a fast FDS able to detect the quick changes in the measured signal. It is found that the discrete wavelet transform (DWT), developed by Mallat,[22] is a valuable tool applied to signals of temperature measurement. It can be decomposed in low- and high-pass multiresolution filters. These filters are defined as functions of a selected wavelet family as well as of its corresponding scaling function (more details can be found in ref 22).

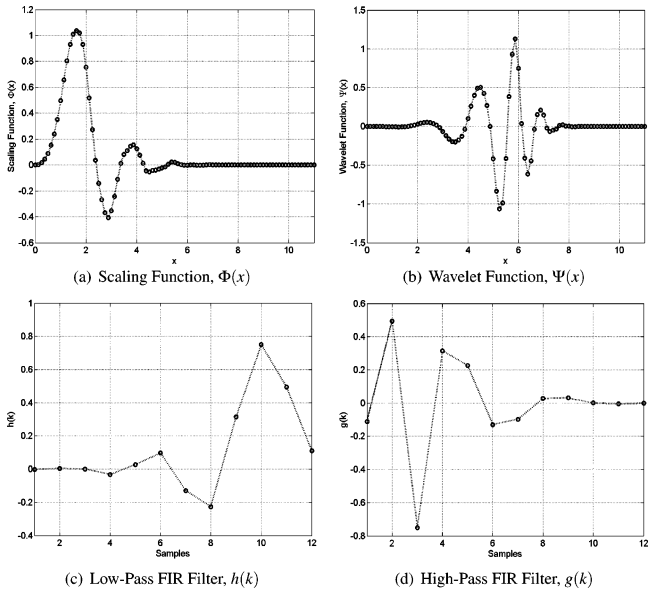


(a) Scaling Function, $\Phi(x)$ (b) Wavelet Function, $\Psi(x)$

(c) Low-Pass FIR Filter, $h(k)$ (d) High-Pass FIR Filter, $g(k)$

**Figure 6.** Daubechies wavelet family of sixth order.

In the wavelet transform, the basis functions are little waves called *wavelets*. They are a family of basis functions whose time-frequency localization or scale are unique in the entire time-frequency domain. Thus, wavelets present multiscale character and are able to adjust their scale to the nature of the signal features. The term wavelet refers to the sets of functions given by

$$\Psi_{d,t}(x) = |d|^{-1/2}\Psi\left(\frac{x-t}{d}\right) \tag{37}$$

They are formed by the dilations, which are controlled by the positive real number $d$, and the translations, which are controlled by the real number $t$, of a single function $\Psi(x)$ often recognized as the mother wavelet. Visually, the mother wavelet appears as a local oscillation. If the dilation and translation parameters $d$ and $t$ are chosen as $d = 2^j$ and $t = k2^j$, where $j$ and $k$ are integers, then there exist wavelets $\Psi(x)$ such that the set of functions given by eq 37 constitute an orthonormal basis of the space of functions or signals that have finite energy.

This transform can be implemented as low- and high-pass multiresolution filters of the measured signal (the Mallat algorithm).[22] The Mallat algorithm for DWT is, in fact, a classical scheme for the signal-processing community, known as a two-channel subband coder using quadrature mirror filters (QMF). These filters are specifically designed and are functions of the selected wavelet family $\Psi(x)$ as well as of its corresponding scaling function $\Phi(x)$. In other words, the localization for both time and frequency domains of the scaling $\Phi(x)$ and wavelet $\Psi(x)$ functions can be chosen by selecting correctly the quadrature mirror filters $h(k)$ (low-pass FIR filter) and $g(k)$ (high-pass FIR filter). The low and high-pass filtering versions are called approximation signal $A$ and detail signal $D$, respectively.

Fortunately, numerous family types of wavelet and scaling functions are available; some of them are as follows: Harr, Daubechies, Morlet, Meyer, and Mexican Hat. For more details to obtain a new wavelet basis, see the paper by Mallat.[22] In Figure 6 is presented the Daubechies wavelet family of sixth order.

The Mallat algorithm is presented in Figure 7. For a given level $j$ (Figure 7a), this algorithm makes the low- and high-pass filtering by convolving the approximation at level $j$ ($A_j$)

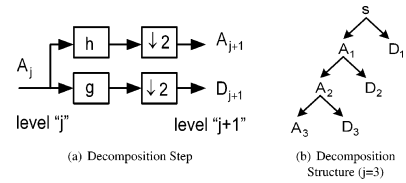


(a) Decomposition Step (b) Decomposition Structure (j=3)

**Figure 7.** Multiresolution filtering (Mallat algorithm).

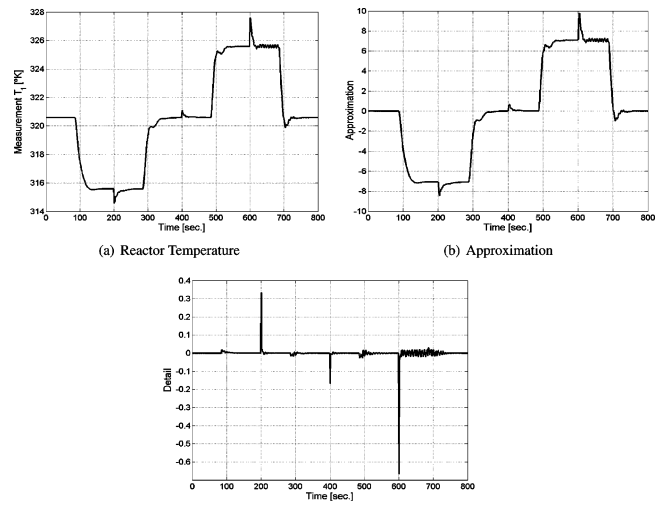


(a) Reactor Temperature (b) Approximation

(c) Detail

**Figure 8.** Wavelet decomposition at level $j = 1$ with Daubechies family of third order.

with the FIR filters $h(k)$ and $g(k)$, respectively. It follows this by doing a downsampling of two (keeping the even indexed elements), which generates the approximation and details signals at level $j + 1$, $A_{j+1}$ and $D_{j+1}$, respectively. The decomposition tree when $j = 3$ is shown in Figure 7b, where $s$ is the original signal.

For the application considered here, the Daubechies wavelet family of third order was used and the decomposition scale was selected to be equal to one. The Mallat algorithm is applied to the reactor temperature measurement ($T_1$) shown in Figure 8. Three arbitrary sensor offsets have been introduced in a step change emulating a faulty behavior: at $t = 200$ s, an offset of $-1$ K; at $t = 400$ s, and offset of 0.5 K; and at $t = 600$ s, an offset of 2 K. Then the reactor temperature measurement in Figure 8a is analyzed via a multiresolution filter up to level 1. Figure 8b shows the low-pass filter output, called approximation at level 1 from the input signal, and Figure 8c shows the high-pass filter output, which has information about the details of this signal (named details at level 1). The detail signal pictures give precise information about the magnitude and direction of the sensor offset present in the signal. This information is used to make proper corrections on the temperature set point, according to the FDS recommendation, in order to compensate this sensor faulty behavior.

Because the wavelet transform is a multiresolution filtering, it is possible to obtain different approximations from the same original signal. Each approximation or details at different scales maximize or minimize the original frequency content of the signal. Thus, details at high scales will be rich in high-frequency content, and the respective approximations will be rich in low-frequency content (coarse version). The faults in the sensor considered here as abrupt bias (like step change) produces a transient process response with high-frequency content, which can be isolated by some details scale. On the other hand, process disturbances are rejected by the controller according to the dynamic system characteristics (nonabrupt), like set-point track-

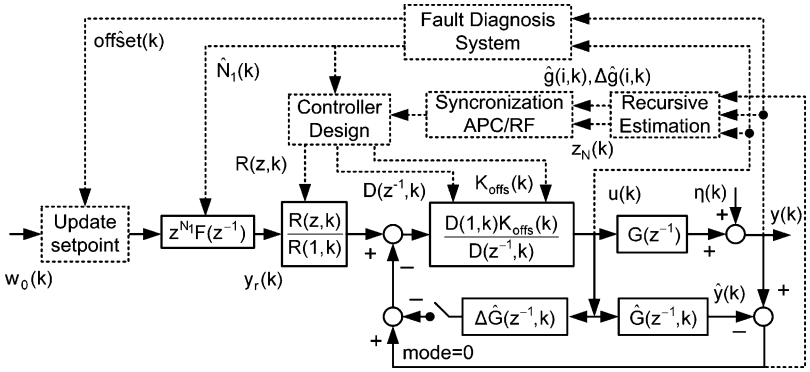


**Figure 9.** FDS integrated to robust adaptive predictive fault-tolerant control.

ing. Thus, its high-frequency content results in being enough lower than that produced by the fault to be easily recognized as an abnormal event by the FDS. In Section 5, where different tests are performed, it will be demonstrated how DWT is able to distinguish perfectly between the set-point changes, the disturbances, the additive noise, etc. with respect to the sensor fault effects analyzed in the scale of the detail chosen for this example. The multiresolution decomposition can isolate the noise effect in other details, depending on the frequency content. Each time that the ratio between noise and signal is very closed will produce a more difficult fault detection and identification.

**4.3. Integration To Active FTC.** In this section, both the system-identification and signal-processing techniques described above are used for developing the reliable FDS able to be integrated with the control structure working in the process. This integration with the APCWRF results in an active FTC strategy, improving the overall performance and the safety conditions of the plant. In Figure 9, the active FTC scheme is shown.

The control algorithms are based on the tracking error between set-point policy and process output (or its predictions, for model based); in other works, the control signal $u(k)$ is a specific function $F(.)$ of this tracking error, such that $u(k) = F(sp(k) - y(k))$. If the measured output is wrong because it is influenced by a bias, $y(k) = y_{true}(k) +$ bias, then the control algorithm will reject this bias similarly as when a disturbance at the output occurs and tries to achieve a zero tracking error as quick as possible; the fault effect virtually disappears from the measured signal, as is shown in Figure 8a. Some possible solutions could be as follows:

(i) additive compensation to the output measurement $y(k)$ with the identified bias;

(ii) additive compensation to the estimation $\hat{y}(k)$, avoiding the plant−model mismatch (disturbance estimation);

(iii) additive compensation to the set-point policy online according to the bias magnitude.

This last approach is performed in the case study analyzed here with certain advantages such as (i) from the monitoring point of view, the set-point update can be more informative and (ii) this approach is independent of the control algorithm that is used. Even though a single-input, single-output (SISO) case is tested in this work, the extension to a multivariable plant model could be done supported by an advanced control structure such as model predictive control (MPC). The set-point updating drives the system to another working point caused by the faulty measurement, maintaining the real process output variable inside the expected working range.

In Figure 8c can be observed the signatures (patterns) caused by three different fault magnitudes (−1 K, 0.5 K, and 2 K), which sequentially occur. These patterns contain the information about the direction and magnitude of the faults. As can be observed, positive deviations (pics) correspond to negative bias in the sensor and vice versa. On the other hand, it is experimentally checked that the absolute value reached by the peak, |peak|, is directly related to the magnitude of the present fault. Thus, a mapping can be performed to estimate the fault magnitude. For the example studied here, this mapping is a linear relationship by means of the proportional factor $\delta$, expressed as $\hat{o}(k) = \delta|\text{peak}|$. Therefore, both the magnitude and the sign estimation are given by the DWT, and this information is used to redefine a new set-point (reference) policy according to eq 38

$$w(k) = w_0(k) + \hat{o}(k) \tag{38}$$

where $w_0(k)$ is the original reference trajectory and $\hat{o}(k)$ is the actual sensor-fault (offset) estimation given by the FDS.

On the other hand, the coolant valve faults (extra delay by mechanical malfunction) are detected and estimated by the FDS using system-identification techniques (delay estimation); the correct delay estimation is used for reconfiguring the control parameters by means of the starting point for the prediction horizon according to eq 39

$$\hat{N}_1(k) = \hat{d}(k) + 1 \tag{39}$$

where $\hat{d}(k)$ is the delay estimation.

In this case, $N_1 = \hat{N}_1(k)$ is assumed, allowing the controller matrix reconfiguration such as, $\mathbf{T}_1$, $\mathbf{T}_3$, $\mathbf{T}_4$, and $\mathbf{A}$. In other words, an alternative way of control law updating is accounted. Therefore, the first update is made by the control scheme via recursive FIR model estimation (*dynamic update*), and the second is done via prediction horizon actualization (*orders update*) with the help of the FDS integrated to the control structure. The FIR modeling used in the control structure corresponds to the input−output (coolant flow−reaction temperature) process model. On the other hand, the ARX modeling between control signal and coolant flow, used in the FDS design, models the valve at normal behavior.

In the multivariable scenario, those critical sensors could include a particular wavelet multiresolution decomposition according to the signal to be processed. Thus, when an offset occurs, the information is given in order to compensate by the set-point trajectory. By means of the discrete-valve model, a continuous monitoring is performed. Thus, any modification in the true delay of the valve is detected, estimated, and reported online. This approach can be extended to the multivariable case, simply monitoring at least the most critical actuators. In both cases, the specific plantwide control structure must be accounted. A similar strategy has been tested with good results on the most complex multivariable plants, such as wastewater treatment[23]

**Table 2. Controller Parameters Settings**

| approach | $T_s$ | $N$ | $N_1$ | $N_2$ | $N_u$ | $\alpha_r$ | **A** | **B** | $\lambda$ |
|---|---|---|---|---|---|---|---|---|---|
| APC/APCWRF | 2 | 20 | 3 | 7 | 1 | 0.001 | diag(1, ..., 1) | 0.65/0 | 0.99/0.95 |

**Table 3. FDS Parameters Settings**

| approach | $T_s$ | wavelet family | decomposition level | $N_w$ | $a_1$ | $a_2$ | $\delta$ |
|---|---|---|---|---|---|---|---|
| APC/APCWRF | 1 | Daubechies, 3rd order | 1 | 200 | 0.0067 | 0.9933 | 3 |

and pulp mill process,[24] where decentralized control structure was implemented.

## 5. Simulation Results

In this section, a proposed set of simulations for visualizing the operation of the FTC strategy is discussed. For the sake of comparison, the behavior of the APC and APCWRF with and without FDS integration was evaluated considering that both reactor temperature sensor and coolant valve faults occur. The simulations have been performed by considering the controller parameters for the APC and APCWRF are those shown in Table 2. The FDS design is implemented accounting the parameters shown in Table 3. Because of the integration with the FDS, the active FTC scheme is available; then some controller parameters are modified when specific abnormal events occur. In the FTC case, $N_1 = \hat{N}_1(k)$ and $N_2 = \hat{N}_1(k) + 4$, where $\hat{N}_1(k)$ is estimated by the FDS.

First, in Figure 10, the responses of both APC and APCWRF approaches can be appreciated when the process is working at a normal condition. In parts a and b of Figure 10, the reactor temperature (controlled variable) and the coolant flow to the jacket (manipulated variable), respectively, can be seen for a variable reference policy. In parts c and d of Figure 10 can be seen the same variables and the regulation effect of the controller when a step disturbance of $\Delta T_{\mathrm{inA}} = -2$ K at $t = 400$ s occurs. The APC strategy demonstrates more aggressive control actions than the APCWRF approach, even though it improves the robustness conditions. Both approaches show a good disturbance rejection.

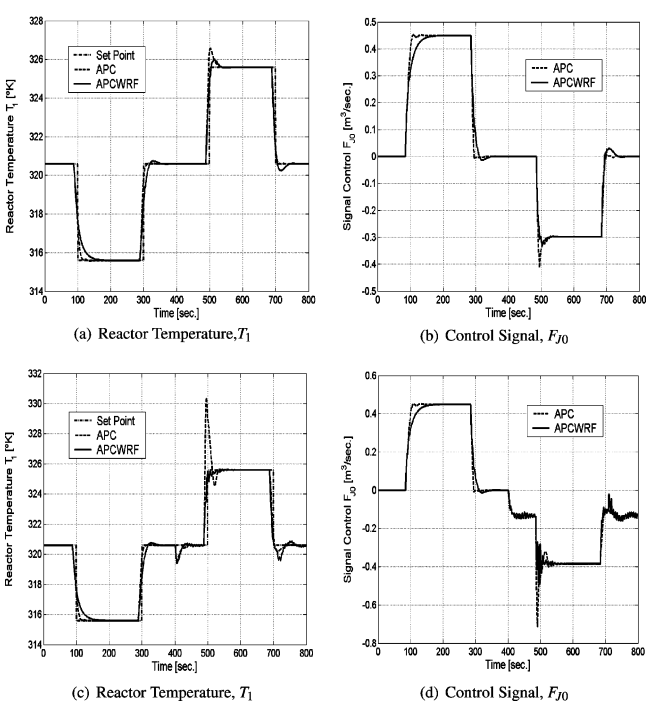


(a) Reactor Temperature, $T_1$ (b) Control Signal, $F_{J0}$

(c) Reactor Temperature, $T_1$ (d) Control Signal, $F_{J0}$

**Figure 10.** APC and APCWRF approach: Normal (a,b) and disturbanced behavior (c,d).

In Figure 11 can be observed the controlled system behavior implementing APC, with and without FDS, when a valve fault of an extra delay of 10 s at $t = 0$ takes place. In parts a and b of Figure 11 can be appreciated the controlled and manipulated variables behavior, respectively. Without FDS information, the dynamic update via recursive FIR estimation only can guarantee stability for some specific reference trajectory. For those zones where the control strategy itself is not able to update the model, the FDS provides the information for adopting a new $N_1$ (Figure 11c) and allows one to stabilize the control loop, improving the global performance. Additionally, Figure 11c shows the correct fault detection done in time and magnitude by the FDS.

Analogously, Figure 12 shows the dynamic behavior of the process controlled by APCWRF strategy, with and without FDS. In this case, the magnitude of the fault is greater than that in the previous case, delay = 15 s at $t = 0$, thanks to the superior robustness characteristics of the APCWRF in comparison to the APC approach; a clear advantage is demonstrated since the correct setting of $N_1$ improves the tracking performance. In parts a and b of Figure 12, the controlled and manipulated profiles are shown for this fault type, respectively, while in Figure 12c, the delay estimation given by the FDS is presented.

In both APC and APCWRF approaches with FDS, the coolant valve fault has been quickly detected and estimated (Figures 11c and 12c) in the transient response, allowing a suitable prediction horizon update. It can be seen how this update makes an effective improvement for analyzing the integral absolute error (IAE $= \int_{t_1}^{t_2} |e(t)|\, \mathrm{d}t$) between the reference trajectory policy and the controlled process variable; see Table 4.

In Figures 13 and 14, the behavior of the controlled process variable with APC and APCWRF approaches, respectively,

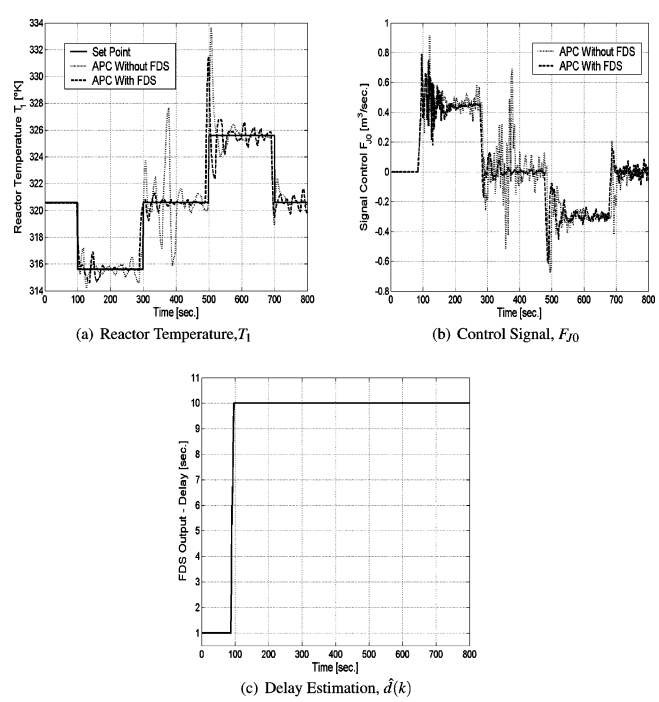


(a) Reactor Temperature, $T_1$ (b) Control Signal, $F_{J0}$

(c) Delay Estimation, $\hat{d}(k)$

**Figure 11.** APC approach (coolant valve fault with and without FDS).

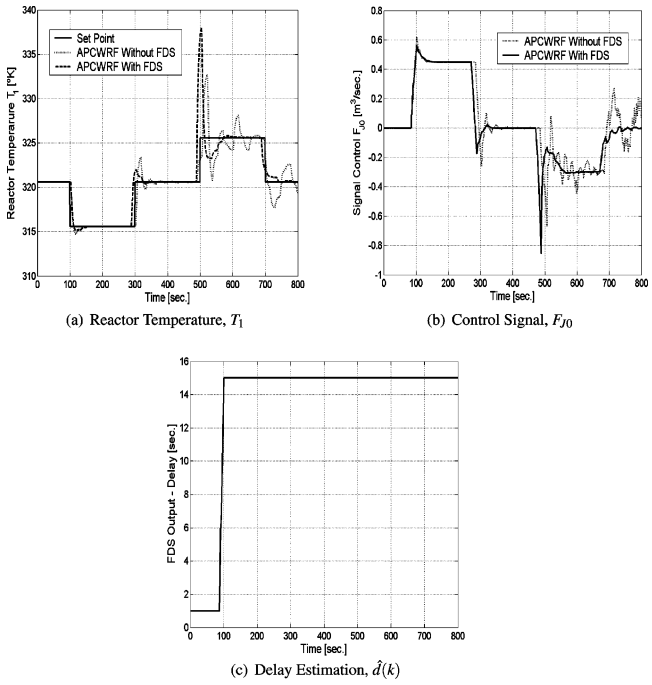


(a) Reactor Temperature, $T_1$ (b) Control Signal, $F_{J0}$

(c) Delay Estimation, $\hat{d}(k)$

**Figure 12.** APCWRF approach (coolant valve fault with and without FDS).

**Table 4. Performance for Fault in Valve**

| approach | APC ($d = 10$ s) | | APCWRF ($d = 15$ s) | |
|---|---|---|---|---|
| with FDS | no | yes | no | yes |
| IAE | 5.99 | 4.09 | 5.70 | 4.72 |

when a fault in the temperature sensor appears can be analyzed with and without FDS. At $t = 400$ s, the temperature measurement presents an abrupt offset of 2 K.

In the APC structure, Figure 13d shows the correct and quick offset estimation given by the FDS. This technique for updating allows the adoption of the reference trajectory policy in a suitable way. The APC with and without FDS (parts a and b of Figure 13, respectively) approaches do not present greater differences with respect to stability conditions. The substantial enhancement of this reference update is based essentially on the possibility of rejecting the effect of the sensor offset in the indirectly controlled variable, the composition $C_A$ (see Figure 13e). This additive fault compensation allows one to return the $C_A$ composition into the normal values and, thus, to maintain the output product quality under specifications.

In Figure 14 can be seen the results obtained when the APCWRF approach is implemented. Parts a and b of Figure 14 show the controlled variable dynamic responses with and without FDS, respectively, for the same sensor fault type. The APCWRF approach presents more robust characteristics than the APC structure. In addition, the time evolution of the variables shows a smooth behavior without oscillations. Again, from Figure 14d is demonstrated the correct offset detection and estimation from the faulty measurement. In this case also, the reference compensation allows for the return of the $C_A$ composition into the normal operating values (Figure 14e).

Another test is included and shown in Figure 15, where one can observethe overall FTC (APCWRF) approach behavior when disturbances and sensor faults are present sequentially. At $t = 200$ s, an arbitrary disturbance in $T_{inA}$ appears with a value of $-2$ K. Then at $t = 400$ s appears a sensor fault of 2 K. In parts a and b of Figure 15 can be observed the effect of these events on temperature reactor measurement without and with FTC approach, respectively. The disturbance is rejected perfectly in both cases, but similarly to the previous simulations,

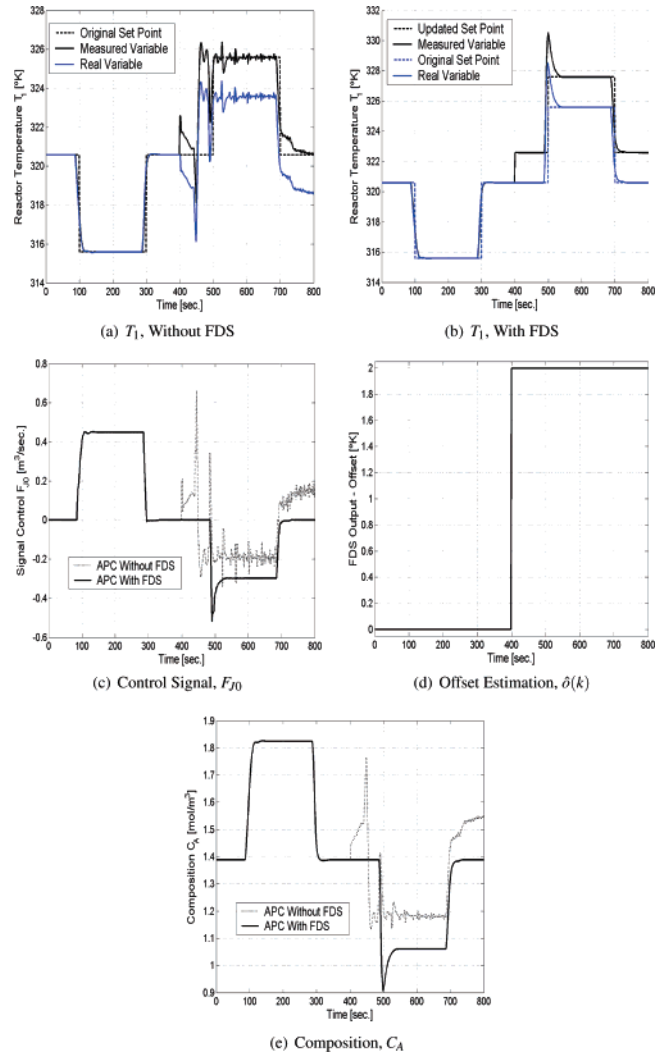


(a) $T_1$, Without FDS (b) $T_1$, With FDS

(c) Control Signal, $F_{J0}$ (d) Offset Estimation, $\hat{\delta}(k)$

(e) Composition, $C_A$

**Figure 13.** APC approach (temperature sensor fault with and without FDS).

the main difference is noticed in the fault management. Without FDS information, the indirectly controlled variable $C_A$ in Figure 15e moves toward another operation point; on the other hand, with the correct fault magnitude estimation shown in Figure 15d, the set-point policy can be corrected on line and the fault is compensated. In Figure 15f, the wavelet decomposition (detail at level 1) is presented; here it is clearly demonstrated that this methodology can distinguish quite well among different events, such as set-point changes, disturbance effects, and abnormal situations, without losing the correct isolation and estimation properties.

The last simulation result considers the disturbance effect and faults appearing in a sequential way applied to the APCWRF algorithm. Figure 16 shows the variables evolution when different abnormal events occur. In this case, the reactor temperature measurement is affected by additive white noise with a power of 0.01. At $t = 100$ s, the valve begins to fail, producing an extra delay of 15 s between when the control signal is generated and when the corresponding coolant flow obeys it. At $t = 200$ s appears a nonmeasured disturbance of $T_{inA} = -2$ K, and finally, a sensor fault at $t = 400$ s occurs of 2 K. In Figure 16a can be seen the APCWRF algorithm without FDS behavior, so the faults are not compensated. The oscillatory behavior produced by the disturbance effect and because of the uncompensated extra time delay can be observed. On the other hand, because the sensor fault is not compensated, the real temperature displacement to another working point is recorded.

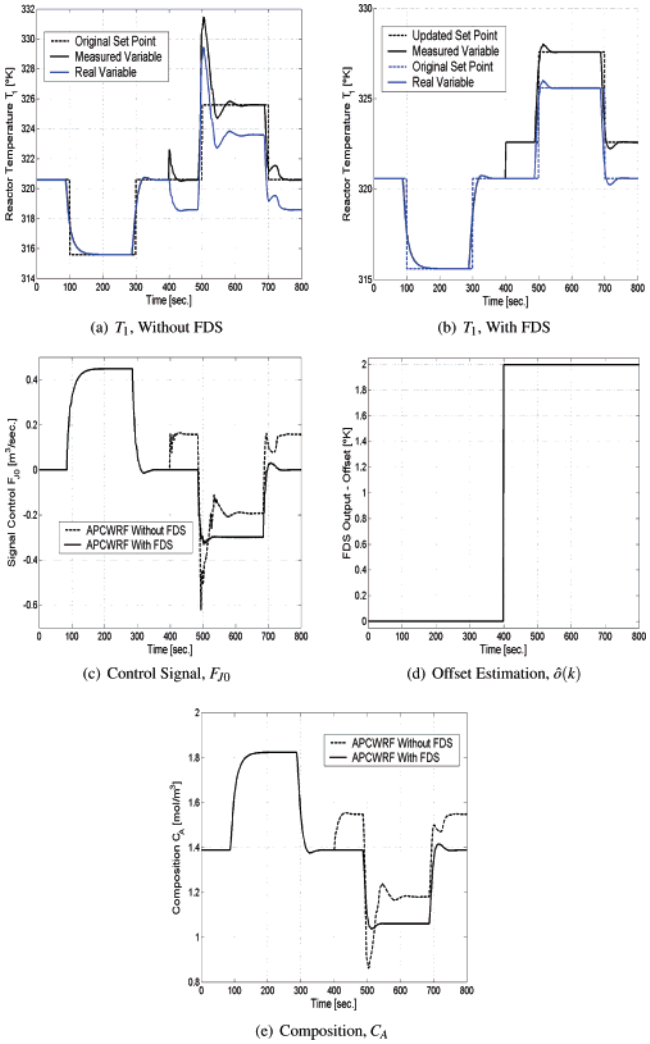


**Figure 14.** APCWRF approach (temperature sensor fault with and without FDS).

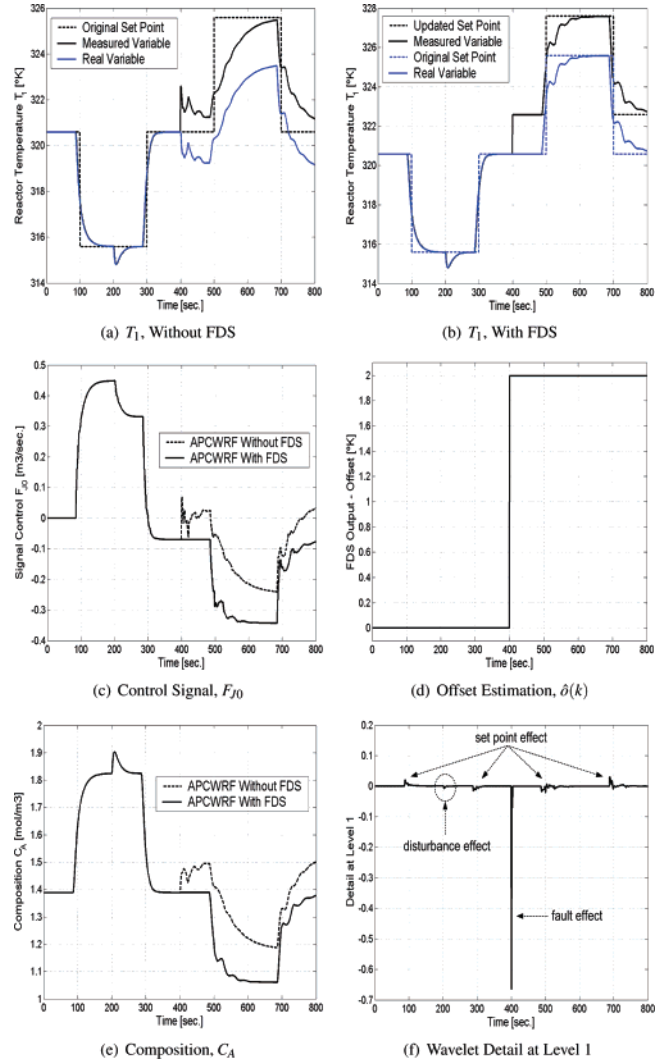


**Figure 15.** APCWRF approach (temperature sensor fault and disturbance with and without FDS).

In Figure 16b, these faults are compensated by integrating the FDS to APCWRF. Here, the oscillations due to disturbance rejection are smaller, since the valve fault is compensated with the delay estimation given by FDS and reconfiguring the controller properly. In addition, the sensor fault is compensated through the set-point policy based on the offset estimation given by the FDS. Thus, the true value of temperature returns to its normal point. In parts c and d of Figure 16, the FDS outputs are included (the delay and bias estimation, respectively). On the other hand, in Figure 16e can be observed how $C_A$ is kept under specification. The APCWRF approach with FDS integration shows how the process management is correctly done even though different abnormal events sequentially occur. In Figure 16f, it can be seen that the noise effect is negligible by the wavelet-decomposition approach. Here, the detail at level 1 is shown; it is demonstrated to be enough for properly isolating the fault impact. In the case of the important noise effect, the decomposition approach must be made by accounting more levels and/or analyzing among other different wavelet families for searching which levels minimize the noise influence and allow one to isolate the fault effect.

The benefit of accounting with the FDS integrated with the FTC is evident from the application results given in this work. On the one hand, the FTC system allows one to improve and guarantee the stability and safety conditions of the controlled process when variable delays are present in the control loop. On the other hand, the sensor faults are compensated properly, keeping the correct output quality performance of the controlled variables.

## 6. Conclusions

In this paper, a new FTC structure is shown enhanced with the integration of a new data-driven FDS. According to the simulation results given previously, it is demonstrated that the robust filter included in the adaptive predictive control strategy allows one to account with a good alternative in the field of active FTC strategy based on APCWRF algorithm. The design integrated with the efficient FDS detailed here significantly improves the overall performance of the controlled nonlinear plant. This is because of its capacity of quantifying the fault magnitude. This system allows the detection and estimation of typical faults at the temperature sensor and at the flow actuator. The FDS used here is demonstrated to be able to isolate and estimate correctly, even with the existence of noisy signals, in the presence of unmeasured disturbances and sequential faults, without producing false alarms. These important characteristics make the FDS very useful for updating the controller parameters online. The sensor bias is detected efficiently by using wavelet decomposition only, without any other procedure. In addition, a new solution for the real problem of variable time delay in the process industry is handled thanks to the FDS integration.

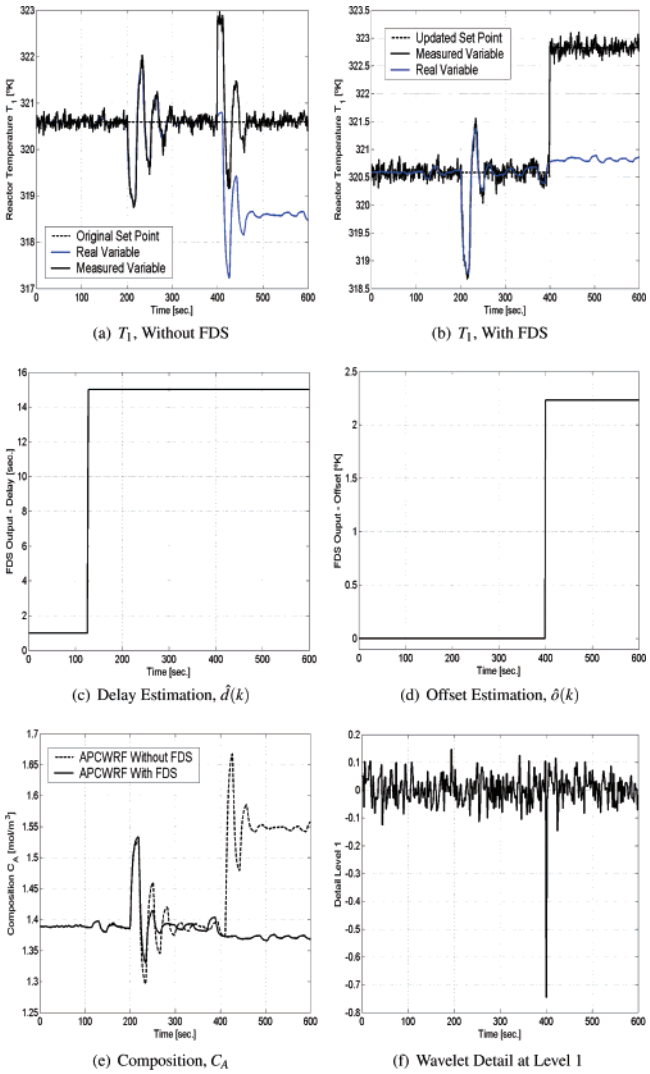


**Figure 16.** APCWRF approach (noisy measurement, actuator fault, and sensor fault with and without FDS).

On the basis of the great number of simulation tests, it is confirmed that the link with the FDS certainly drives to an interesting improvement on safety and economical features. Hence, as future works, the extension to large multivariable complex chemical plants are planned to be tested with the most common faults in practice and for different FTC strategies.

## Acknowledgment

The authors want to acknowledge the National Council of Scientific and Technological Research (CONICET) of Argentina and ANPCyT under PICT 11-11150.

## Literature Cited

(1) Venkatasubramanian, V.; Rengaswamy, R.; Yin, K.; Kavuri, S. N. A Review Of Process Fault Detection And Diagnosis. Part I: Quantitative Model-Based Methods. *Comput. Chem. Eng.* **2003**, *27*, 293−311.

(2) Venkatasubramanian, V.; Rengaswamy, R.; Kavuri, S. N. A Review Of Process Fault Detection And Diagnosis. Part II: Qualitative Models And Search Strategies. *Comput. Chem. Eng.* **2003**, *27*, 313−326.

(3) Venkatasubramanian, V.; Rengaswamy, R.; Kavuri, S. N.; Yin, K. A Review Of Process Fault Detection And Diagnosis. Part III: Process History Based Methods *Comput. Chem. Eng.* **2003**, *27*, 327−346.

(4) Luo, R.; Misra, M.; Himmelblau, D. Sensor Fault Detection via Multiscale Analysis and Dynamic PCA. *Ind. Eng. Chem. Res.* **1999**, *38*, 1489−1495.

(5) Richard, J. P. Time-Delay Systems: An Overview Of Some Recent Advances And Open Problems. *Automatica* **2003**, *39*, 1667−1694.

(6) Wei, G.; Guang-Fu, M.; Miao-Lei, Z.; Yuan-Chun, L.; Ying, L. Parameter Identification And Adaptive Predictive Control Of Time-Varying Delay Systems. In *Proceedings of the Fourth International Conference on Machine Learning and Cybernetics*, Guangzhou, China, 2005; pp 609−613.

(7) Jiang, C.; Zhou, D. H. Fault Detection And Identification For Uncertain Linear Time-Delay Systems. *Comput. Chem. Eng.* **2005**, *30*, 228−242.

(8) Zhou, D. H.; Frank, P. M. Fault Diagnostics and Fault Tolerant Control. *IEEE Trans. Aerospace Electron. Syst.* **1998**, *34*, 420−427.

(9) Campos-Delgado, D.; Zhou, K. Reconfigurable Fault-Tolerant Control Using GIMC Structure. *IEEE Trans. Automatic Control* **2003**, *48*, 832−838.

(10) Tao, G.; Chen, S.; Joshi, S. M. An Adaptive Actuator Failure Compensation Controller Using Output Feedback. *IEEE Trans. Automatic Control* **2002**, *47*, 506−511.

(11) Zhang, X.; Parisini, T.; Polycarpou, M. M. Adaptive Fault-Tolerant Control of Nonlinear Uncertain Systems: An Information-Based Diagnostic Approach. *IEEE Trans. Automatic Control* **2004**, *49*, 1259−1274.

(12) El-Farra, N. H. Integrated Fault Detection and Fault-Tolerant Control Architectures for Distributed Processes. *Ind. Eng. Chem. Res.* **2006**, *45*, 8338−8351.

(13) Patwardhan, S. C.; Shah, S. L. From data to diagnosis and control using generalized orthonormal basis filters. Part I: Development of state observers. *J. Process Control* **2005**, *15*, 819−835.

(14) Patwardhan, S. C.; Manuja, S.; Narasimhan, S.; Shah, S. L. From data to diagnosis and control using generalized orthonormal basis filters. Part II: Model predictive and fault tolerant control. *J. Process Control* **2006**, *16*, 157−175.

(15) Prakash, J.; Patwardhan, S. C.; Narasimhan, S. A Supervisory Approach to Fault-Tolerant Control of Linear Multivariable Systems. *Ind. Eng. Chem. Res.* **2002**, *41*, 2270−2281.

(16) Jordán, M.; Basualdo, M.; Zumoffen, D. An Approach to Improve the Performance of Adaptive Predictive Control Systems: Theory, Simulations and Experiments. *Int. J. Control* **2006**, *79*, 1216−1236.

(17) Jordán, M. Digitale Adaptive Regelung mit linearen nichtparametrischen Modellen. Ph.D. Thesis, Technische Hochschule Darmstadt, Düsseldorf, Germany, 1991.

(18) Bjorklund, S.; Ljung, L. A Review Of Time-Delay Estimation Techniques. In *Proceedings of 42nd IEEE Conference on Decision and Control*, Maui, HI, Dec 2003; pp 2502−2507.

(19) Ljung, L. *System Identification, Theory For The User*; Prentice Hall: Upper Saddle River, NJ, 1999.

(20) Kofahl, R. *Robustness in Parameter Adaptive Control. Chapter XIII In Adaptive Control Systems*; Isermann, R., Lachmann, K. H., Matko, D., Eds.; Prentice Hall: New York, 1992.

(21) Primucci, M.; Basualdo, M. Thermodynamic Predictive Functional Control Applied To CSTR With Jacket System. In *Proceedings of IFAC World Congress*, Barcelona, Spain, 2002.

(22) Mallat, S. G. A Theory for Multiresolution Signal Decomposition: The Wavelet Representation. *IEEE Trans. Pattern Anal. Machine Intelligence* **1989**, *II*, 674−693.

(23) Zumoffen, D.; Basualdo, M. Fault Detection and Estimation System Integrated To Fault Tolerant Control: WasteWater Treatment Plant Application. Submitted for publication.

(24) Zumoffen, D.; Basualdo, M. From Large Chemical Plant Data to Fault Diagnosis Integrated To Decentralized Fault Tolerant Control: Pulp Mill Process Application. Submitted for publication.

*Received for review* January 5, 2007
*Revised manuscript received* July 31, 2007
*Accepted* August 3, 2007

IE070019B